iScience, Volume *23*

Supplemental Information

Incorporation of a Novel CD4+ Helper Epitope Identified from *Aquifex aeolicus* Enhances Humoral Responses Induced by DNA and Protein Vaccinations

Ziyang Xu, Neethu Chokkalingam, Edgar Tello-Ruiz, Susanne Walker, Daniel W. Kulp, and David B. Weiner

Supplemental Figures and Table

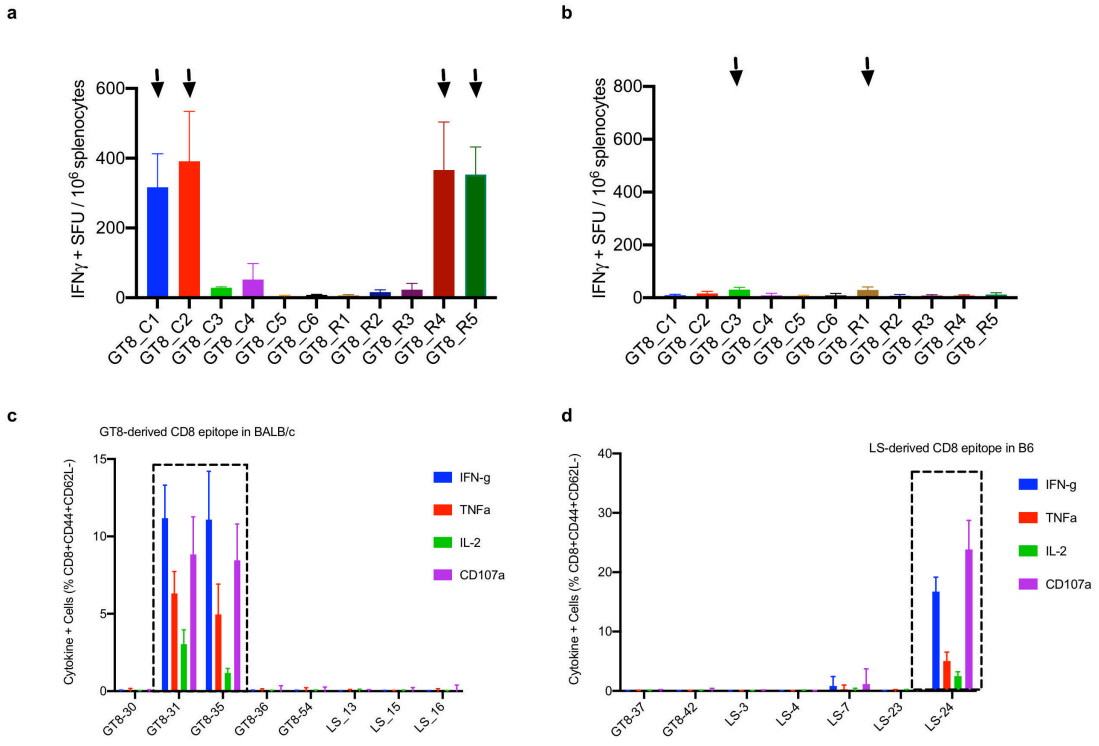

Figure S1. CD8+ T-cell epitopes in DLnano_LS_GT8 were mapped to the GT8 and LS domains in BALB/c and C57BL/6 mice, respectively. **Related to Figure 1.** Mice received 25ug DNA vaccination with EP twice three weeks apart and were euthanized two weeks post the second vaccination for cellular analysis. **a** and **b**. Matrix mapping by IFNγ ELISpot assays in the GT8 domain to determine the dominant T-cell epitopes in BALB/c (**a**) or C57BL/6 (**b**) mice. **c**. and **d.** Identification of the dominant CD8+ T-cell epitope by ICS in the GT8 domain for BALB/c mice (**c**) and in the LS domain for C57BL/6 mice (**d**). Each group includes five mice; error bar represents standard deviation; arrow above the bar graph represents the dominant peptide pool identified.

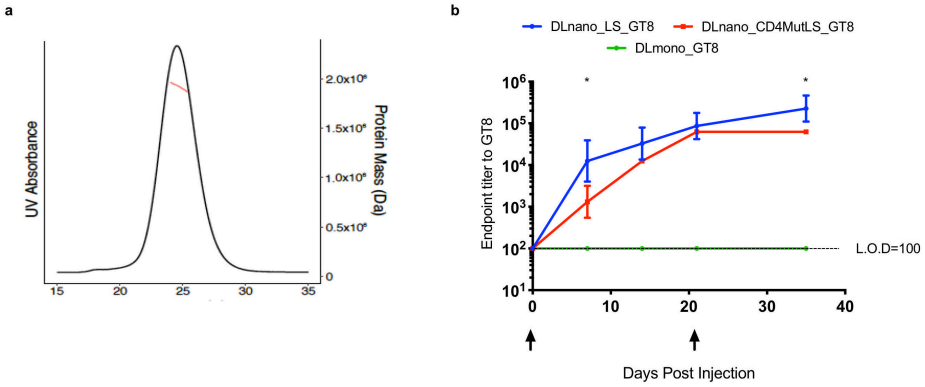

Figure S2. Knock out of the LS-3 epitope from DLnano_LS_GT8 was observed to attenuate vaccine-induced humoral immunity. **Related to Figure 3.** Mice were immunized in the same manner as described in **Figure 3a.** SEC-MAL trace of SEC-purified CD4MutLS_GT8; the molecular weight was determined to be around 2MDa for CD4MutLS_GT8. **b.** Humoral responses induced to GT8 by two doses of DLnano_CD4MutLS_GT8 in comparison to DLnano_LS_GT8 and DLmono_GT8, as assessed by ELISA; p-values compare differences between DLnano_CD4MutLS_GT8 and DLnano_LS_GT8 at each timepoint. Each group includes five mice; error bar represents standard deviation; two-tailed Mann-Whitney Rank Test used to compare groups; *, p-value<0.05.

a

Peptide	PADRE	LS3
Number of Residues	13	15
Molecular Weight g/mol	1348	1624
Iso-electric point (pH)	10.7	12.1
Net Charge at pH 7	2.0	2.1
Water solubility	Poor	Poor

b

Peptide: PADRE- AKFVAAWTLKAAA				
	allele	smm_align_ic50 (nM)	nn_align_ic50 (nM)	Measured_ic50 (nM)
Human	HLA-DRB1*07:01	144	17.9	1.2
	HLA-DRB5*01:01	179	11.8	18
	HLA-DRB3*01:01	1262	310.2	1470
Murine	H2-Iab	677	95.8	44

c

	LS3	PADRE	FC_CH1$_{1-15}$
Peptide	LRFGIVASRANHALV	AKFVAAWTLKAAA	ASTKGPSVFPLAPSS
DRB1_01_01 *	0.369	3.66	89.5
DRB1_01_02 *	0.16	9.19	89.3
DRB1_01_03	0.409	0.504	90
DRB1_03_01 *	1.74	12	72
DRB1_04_01	1.16	0.046	15.8
DRB1_04_04 *	0.755	4.72	50.8
DRB1_04_05	6.41	1.97	27.9
DRB1_04_08	1.67	0.0995	16
DRB1_07_01 *	0.63	3.46	73.1
DRB1_08_01	6.53	9.02	90.3
DRB1_10_01	1.52	2.49	57.3
DRB1_11_01	3.75	0.0901	83.1
DRB1_11_04	1.5	1.27	74.2
DRB1_12_01	8.03	17.2	69.9
DRB1_13_01	1.81	2.16	69.4
DRB1_13_03	1.02	3.42	80.3
DRB1_15_01 *	3.12	10.5	31
DRB1_16_01 *	1.31	3.5	67.4
DRB3_01_01 *	2.99	11.6	62.3
DRB3_02_02 *	0.281	12.1	15.3
DRB4_01_01	4.62	12.4	12.5
DRB4_01_03	6.66	13.5	12.9
DRB5_01_01	4.31	10.2	90
DRB5_02_02 *	0.76	6.09	48.3
Geometric mean	1.59	3.08	48.10

Figure S3. LS3 and PADRE epitopes were observed to have complementary coverage in binding to different human HLA-DR alleles. **Related to Figure 4.** **a.** Comparison of predicted biophysical properties between PADRE and LS-3, in terms of molecular weight, isoelectric point, net charge at pH 7 and water solubility. **b.** Comparison of predicted IC50 binding affinities of PADRE epitope to human DRB1_07_01, DRB5_01_01, DRB3_01_01 and murine HLA-Iab by smm-align and nn-align versus reported experimentally measured IC50 binding affinities (Alexander et al., 1994). **c.** Comparison of predicted IC50 binding affinities (in terms of percentile rank, 0-100) of LS-3, PADRE, and Fc-CH1$_{1-15}$ epitopes to various human HLA-DR alleles by MixMHCIIpred (Racle et al., 2019); a lower percentile rank is suggestive of higher binding affinity.

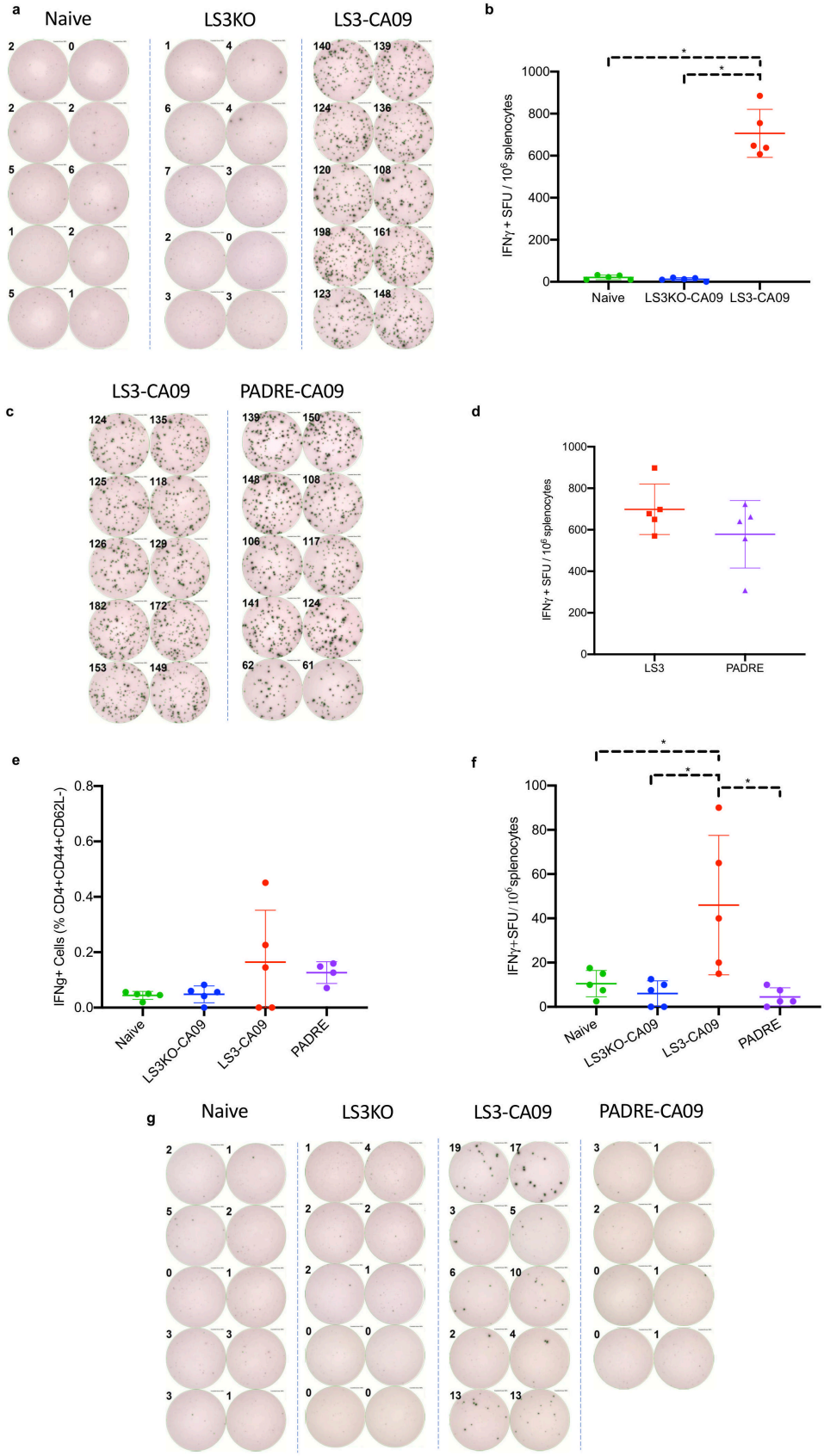
a
Naive
LS3KO
LS3-CA09
2 0
2 2
5 6
1 2
5 1
1 4
6 4
7 3
2 0
3 3
140 139
124 136
120 108
198 161
123 148
b
IFNγ+ SFU / 10^6 splenocytes
1000
800
600
400
200
0
*
*
Naive
LS3KO-CA09
LS3-CA09
c
LS3-CA09
PADRE-CA09
124 135
125 118
126 129
182 172
153 149
139 150
148 108
106 117
141 124
62 61
d
IFNγ+ SFU / 10^6 splenocytes
1000
800
600
400
200
0
LS3
PADRE
e
IFNg+ Cells (% CD4+CD44+CD62L-)
0.8
0.6
0.4
0.2
0.0
Naive
LS3KO-CA09
LS3-CA09
PADRE
f
IFNγ+SFU / 10^6splenocytes
100
80
60
40
20
0
*
*
*
Naive
LS3KO-CA09
LS3-CA09
PADRE
g
Naive
LS3KO
LS3-CA09
PADRE-CA09
2 1
5 2
0 1
3 3
3 1
1 4
2 2
2 1
0 0
0 0
19 17
3 5
6 10
2 4
13 13
3 1
2 1
0 1
0 1

Figure S4. The LS-3 and PADRE epitopes were observed to elicit epitope-specific CD4+ T-cell responses by DNA vaccination, and to a lesser extent, by protein vaccination. Related to Figure 4. C57BL/6 mice received either DNA or protein vaccinations and were euthanized as described in Figure 4. **a** and **b.** IFNγ+ ELIspot assays comparing T-cell responses induced by either DNA-encoded LS3-CA09 or LS3KO-CA09 immunizations in mice to LS3 and LS3KO peptides respectively. **c** and **d.** IFNγ+ ELIspot assays comparing T-cell responses induced by either DNA-encoded LS3-CA09 or PADRE-CA09 immunizations in mice to LS3 and PADRE peptides respectively. **e.** ICS analysis of CD4+ IFNγ+ responses induced by protein LS3KO-CA09, LS3-CA09, or PADRE-CA09 vaccinations in mice to LS3KO, LS3, and PADRE peptides respectively. **f** and **g.** IFNγ+ ELIspot assays comparing T-cell responses induced by protein LS3KO-CA09, LS3-CA09, or PADRE-CA09 vaccinations in mice to LS3KO, LS3, and PADRE peptides respectively. Each group includes five mice; each dot represents a mouse; error bar represents standard deviation; two-tailed Mann-Whitney Rank Test used to compare groups; p-values were adjusted for multiple comparison where appropriate; *, p-value<0.05.

Strain	Category	Domain	Sequence	Classification
BALB/c	CD4	Lumazine Synthase	DAVIAIGVLCRGATP	WT
		Lumazine Synthase	ATPSFDYIASEVSKG	WT
	CD8	GT8	TRQGGYSNDNTVIFR	WT
		GT8	ARCQIAGTVVSTQLF	WT
C57BL/6	CD4	Lumazine Synthase	LRFGIVASRANHALV	WT
		Lumazine Synthase	LKFGIVGSRFNHGLV	LS3KO
	CD8	Lumazine Synthase	AALCAIEMANLFKSL	WT

Table S1. Identified CD4+ and CD8+ epitopes in the LS and GT8 domains in the BALB/c and C57BL/6 mice immunized twice with 25ug DLnano_LS_GT8 three weeks apart and sacrificed two weeks post the second vaccination for cellular analysis. Related to Figure 1.

Transparent Methods

Structure modeling and design of CD4Mut_LS_GT8 nanoparticles

Mutations to the LS-3 peptide were achieved using a structure-guided process. First, positions 14, 19, 22 and 24 in the LS domain were selected for mutation because they were making minimal contacts to the rest of the LS 1HQK crystal structure, which we hypothesized would have less detrimental effect on protein folding. Second, we used the 'fixbb' application of ROSETTA to computationally mutate the selected positions to each of the 20 amino acids allowing neighboring residues to change conformation. Mutations were selected which had similar or lower total score relative to the wild-type amino acid and by visual inspection of the resulting structural models. The mutations were R14K, A19G, A22F, A24G.

DNA design and plasmid synthesis

Protein sequences for IgE Leader Sequence and eOD-GT8-60mer were as previously reported (Briney et al., 2016; Xu et al., 2018). DNA encoding protein sequences were codon and RNA optimized as previously described (Xu et al., 2018). The optimized transgenes were synthesized de novo (GenScript) and cloned into a modified pVAX-1 backbone under the control of the human CMV promoter and bovine growth hormone poly-adenylation signal.

Production of His-Tagged LS3-CA09, LS3KO-CA09, or PADRE-CA09

Expi293F cells were transfected with pVAX plasmid vector carrying the His-Tagged LS3-CA09, LS3KO-CA09, PADRE-CA09, GT8-monomer, eOD-GT8-60mer or CD4Mut_LS_GT8-60mer transgene with PEI/OPTI-MEM and harvested 6 days post-transfection. Transfection supernatant was first purified with affinity chromatography using the AKTA pure 25 system and an IMAC Nickel column for His-Tagged constructs and gravity flow columns filled with GNL Lectin beads (for nanoparticles). The eluate fractions from the affinity purification were pooled, concentrated and dialyzed into 1X PBS buffer before being loaded onto the SEC column and then purified with size exclusion chromatography with the Superdex 200 10/300 GL column (GE Healthcare) for His-Tagged constructs, and with Superose 6 Increase 10/300 GL column for nanoparticles. Identified eluate fractions were then collected and concentrated to 1mg/mL in PBS.

Animals

All animal experiments were carried out in accordance with animal protocols 201214 and 201115 approved by the Wistar Institute Institutional Animal Care and Use Committee (IACUC). For DNA-based immunization, 6 to 8 week old female C57BL/6 or BALB/c mice (Jackson Laboratory) were immunized with DNA vaccines via intramuscular injections into the tibialis anterior muscles, coupled with intramuscular EP with the CELLECTRA 3P device (Inovio Pharmaceuticals). In experiments in Figure 1 and 3, mice were immunized twice with 25ug DNA plasmid three weeks apart and euthanized two weeks post the second vaccination. In experiments in Figure 4, mice were immunized twice with 25ug DNA plasmid twice four weeks apart and

euthanized one week post the second vaccination. For vaccinations involving recombinant protein, 6 to 8-week-old female C57BL/6 mice were immunized intramuscularly with 10ug of recombinant LS3-CA09, LS3KO-CA09 or PADRE-CA09 protein in 15uL sterile PBS co-formulated with 15uL Sigma Adjuvant System (SigmaAldrich) in the tibialis anterior muscles three times four weeks apart and were euthanized one week post the third immunization.

HA-binding ELISA

96-well half area plates were coated at 4C overnight with 2ug/mL of recombinant HA(ΔTM)(A/California/04/2009) (Immune Technology), and blocked at room temperature for 2 hour with a solution containing 1x PBS, 5% skim milk, 10% goat serum, 1% BSA, 1% FBS, and 0.2% Tween-20. The plates were subsequently incubated with serially diluted mouse sera at 37C for 2 hours, followed by 1-hour incubation with anti-mouse IgG H+L HRP (Bethyl) at 1:20,000 dilution at room temperature and developed with TMB substrate. Absorbance at 450nm and 570nm were recorded with BioTEK plate reader.

Antigenic profile characterization of purified eOD-GT8-60mer and CD4Mut_LS_GT8-60mer

Corning half-area 96-well plates were coated with 2ug/mL of purified eOD-GT8-60mer or *CD4Mut_LS_GT8-60mer* at 4C overnight. The plates were then blocked with the buffer as described above for 2 hours at room temperature, followed by incubation with serially diluted VRC01 at room temperature for 2 hours. The plates were then incubated with anti-human Fc (cross-adsorbed against rabbits and mice) (Jackson Immunoresearch) at 1:10,000 dilution for 1 hour, followed by addition of TMB substrate for detection. Absorbance at 450nm and 570nm were recorded with BioTEK plate reader.

HAI assay

Mice sera were treated with receptor-destroying enzyme (RDE, 1:3 ratio; SEIKEN) at 37°C overnight for 18–20 h followed by complement and enzyme inactivation at 56°C for 45 min. RDE-treated sera were subsequently cross-adsorbed with 10% rooster red blood cells (Lampire Biologicals) in 0.9% saline at 4C for 1 hour. The cross-adsorbed sera were then serially diluted with PBS in a 96-well V-bottom microtiter plates (Corning). Four hemagglutinating doses (HAD) of A/California/07/2009 (H1N1)pdm09 (Virapur) were added to each well and the serum–virus mixture was incubated at room temperature for 1 hour. The mixture was then incubated with 50 µl 0.5% v/v rooster red blood cells in 0.9% saline for 30 min at room temperature. The HAI antibody titer was scored with the dot method, and the reciprocal of the highest dilution that did not cause agglutination of the rooster red blood cells was recorded.

ELISpot Assay

Spleens from immunized mice were collected and homogenized into single cell suspension with a tissue stomacher in 10% FBS/ 1% Penicillin- streptomycin in RPMI 1640. Red blood cells were subsequently lysed with ACK lysing buffer (ThermoFisher) and percentage of viable cells were determined with Trypan Blue

exclusion using Vi-CELL XR (Beckman Coulter). 200,000 cells were then plated in each well in the mouse IFNγ ELISpot plates (MabTech), followed by addition of peptide pools that span both the lumazine synthase, 3BVE, PfV or GT8 domains, or individual LS-3, LS3KO or PADRE peptides at 5ug/mL of final concentration for each peptide (GenScript). The cells were then stimulated at 37C for 16-18 hours, followed by development according to the manufacturer's instructions. Spots for each well were then imaged and counted with ImmunoSpot Macro Analyzer.

Intracellular cytokine staining

Single cell suspension from spleens of immunized animals were prepared as described before and stimulated with 5ug/mL of peptides (GenScript) for 5 hours at 37C in the presence of 1:500 protein transport inhibitor (ThermoFisher). The cells were then incubated with live/dead for 10 min at room temperature, surface stains (anti-mouse CD4 BV510, anti-mouse CD8 APC-Cy7, anti-mouse CD44 AF700, anti-mouse CD62L BV771) (BD-Biosciences) at room temperature for 30minutes. The cells were then fixed and permeabilized according to manufacturer's instructions for BD Cytoperm Cytofix kit and stained with intracellular stains anti-mouse IL-2 PE-Cy7, anti-mouse IFN-γ APC, anti-mouse CD3e PE-Cy5 and anti-mouse TNFα BV605 (BioLegend) at 4C for 1 hour. The cells were subsequently analyzed with LSR II 18-color flow cytometer.

Epitope mapping

15-mer peptides spanning the LS and GT8 domains of eOD-GT8-60mer (GenScript) were arranged into row and column pools (each peptide appears exactly once in the row pool and once in the column pool). Splenocytes from BALB/c or C57BL/6 immunized twice with 25ug DLnano_LS_GT8 were co-incubated with each peptide pool with a final concentration of 5ug/mL for each peptide overnight in IFNγ ELIspot plates (MabTech). The plates were then developed according to manufacturer's instruction, and peptides that can potentially stimulate T-cell responses were identified based on the combination of row and column pools that induce IFNγ responses. Responses to those peptides were then confirmed with ICS as described in the last section.

In silico analysis

Binding analysis prediction using smm- and nn-align was performed with a web-based application at the following site (http://tools.iedb.org/mhcii/) (Nielsen and Lund, 2009; Nielsen et al., 2007). Binding analysis prediction using the MixMHCIIpred model was executed with C++ using the codes available at the following site (http://mixmhc2pred.gfellerlab.org/) (Racle et al., 2019).

Statistics

Power analysis was performed with R based on our preliminary data to determine the smallest sample size that would allow us to achieve a power of 0.9 with a pre-set α-value of 0.05. All statistical analyses were

performed with PRISM V8.2.1 and R V3.5.1. Each individual data point was sampled independently. Two-tailed Mann Whitney Rank Tests were used to compare differences between groups. Bonferroni corrections were used to adjust for multiple comparisons.

Supplemental References

Alexander, J., Sidney, J., Southwood, S., Ruppert, J., Oseroff, C., Maewal, A., Snoke, K., Serra, H.M., Kubo, R.T., Sette, A.*, et al.* (1994). Development of high potency universal DR-restricted helper epitopes by modification of high affinity DR-blocking peptides. Immunity *1*, 751-761.

Briney, B., Sok, D., Jardine, J.G., Kulp, D.W., Skog, P., Menis, S., Jacak, R., Kalyuzhniy, O., de Val, N., Sesterhenn, F.*, et al.* (2016). Tailored Immunogens Direct Affinity Maturation toward HIV Neutralizing Antibodies. Cell *166*, 1459-1470 e1411.

Nielsen, M., and Lund, O. (2009). NN-align. An artificial neural network-based alignment algorithm for MHC class II peptide binding prediction. BMC Bioinformatics *10*, 296.

Nielsen, M., Lundegaard, C., and Lund, O. (2007). Prediction of MHC class II binding affinity using SMM-align, a novel stabilization matrix alignment method. BMC Bioinformatics *8*, 238.

Racle, J., Michaux, J., Rockinger, G.A., Arnaud, M., Bobisse, S., Chong, C., Guillaume, P., Coukos, G., Harari, A., Jandus, C.*, et al.* (2019). Robust prediction of HLA class II epitopes by deep motif deconvolution of immunopeptidomes. Nat Biotechnol *37*, 1283-1286.

Xu, Z., Wise, M.C., Choi, H., Perales-Puchalt, A., Patel, A., Tello-Ruiz, E., Chu, J.D., Muthumani, K., and Weiner, D.B. (2018). Synthetic DNA delivery by electroporation promotes robust in vivo sulfation of broadly neutralizing anti-HIV immunoadhesin eCD4-Ig. EBioMedicine *35*, 97-105.